Supplemental material

Enhancement Mechanism of the Conversion Effficiency of Dye-Sensitized Solar Cells Based on N, F, and I-Doped TiO_2 Photoanodes

Mang Niu[a], Rong Cui[b], Hao Wu[b], Daojian Cheng[a,b*], and Dapeng Cao[a,c*]

[a]*State Key Laboratory of Organic-Inorganic Composites, Beijing University of Chemical Technology, Beijing 100029, People's Republic of China*

[b]*Changzhou Institute of Advanced Materials, Beijing University of Chemical Technology, Changzhou 213164, P. R. China*

[c]*International Research Center for Soft Matter, Beijing University of Chemical Technology, Beijing 100029, People's Republic of China*

[*] Authors to whom correspondence should be addressed. Electronic addresses: chengdj@mail.buct.edu.cn and caodp@mail.buct.edu.cn Fax: +8610-64427616

1. The structural properties of N, F and I doped anatase TiO_2.

Figure S1 shows the anatase supercell models of N, F and I doped anatase TiO_2. The incorporated N and F atoms substituted the X1 and X2 O sites, whereas the I dopants substituted the Y1 and Y2 Ti sites of anatase TiO_2. In the geometry optimization, both the lattice constant and the ions position were allowed to be relaxed. The optimized lattice constants of N, F and I doped anatase TiO_2 were listed in Table S1. It is found that the lattice constants of I doped anatase TiO_2 are larger than that of pure anatase TiO_2. The increase of lattice constants can attribute to the lager atom radius of I than that of Ti.

2. The DOSs of N, F and I doped anatase TiO_2.

Figure S2(a) shows that the incorporation of N dopants in anatase TiO_2 induces partially occupied N-2p impurity states above the VBM. The HSE06 calculated band gaps of N doped TiO_2 are 3.142 and 3.013 eV for the low and high N doping concentrations, respectively. Therefore, N doping in TiO_2 can improve the visible-light absorption of TiO_2 but shows minor effect on the band gap reduction. The DOSs plots of F doped anatase TiO_2 indicate that most F-2p states are localized in the lower-energy range of the valence band and do not induce impurity states in the band gap [see Figure S2(b)]. The HSE06 calculated band gaps of F doped TiO_2 are 3.101 and 3.094 eV for the low and high F doping concentrations, respectively. Thus, F doping is not a good choice for extending the optical absorption edge of TiO_2 into the visible-light region. As shown in Figure S2(c), I doping in TiO_2 introduce a fully

occupied band gap state about 1.0 eV above the VBM and thus lead to an effective band gap reduction of TiO_2. The HSE06 calculated band gaps of I doped TiO_2 are 1.922 and 2.131 eV for the low and high I doping concentrations, respectively.

Table S1 The optimized lattice constants (Å) of different kinds of anatase TiO_2.

Structure		Lattice constants		
		a	*b*	*c*
Pure TiO_2		3.821	3.821	9.683
N doped TiO_2	3.125%	3.818	3.837	9.688
	6.25%	3.829	3.832	9.699
F doped TiO_2	3.125%	3.837	3.839	9.640
	6.25%	3.853	3.856	9.602
I doped TiO_2	6.25%	3.854	3.854	9.749
	12.5%	3.888	3.888	9.774

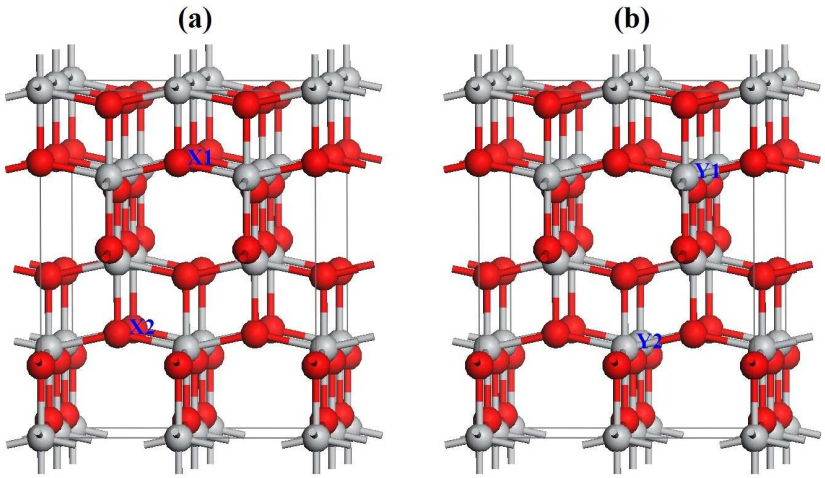

Figure S1. The 2×2×1 anatase TiO_2 supercell models used to simulate (a) N and F doped anatase TiO_2 and (b) I doped anatase TiO_2. The red and the gray spheres represent the O and Ti atoms of TiO_2, respectively. X1 (or Y1) and X1+X2 (or Y1+Y2) represent the dopant sites in the low and high doping levels, respectively.

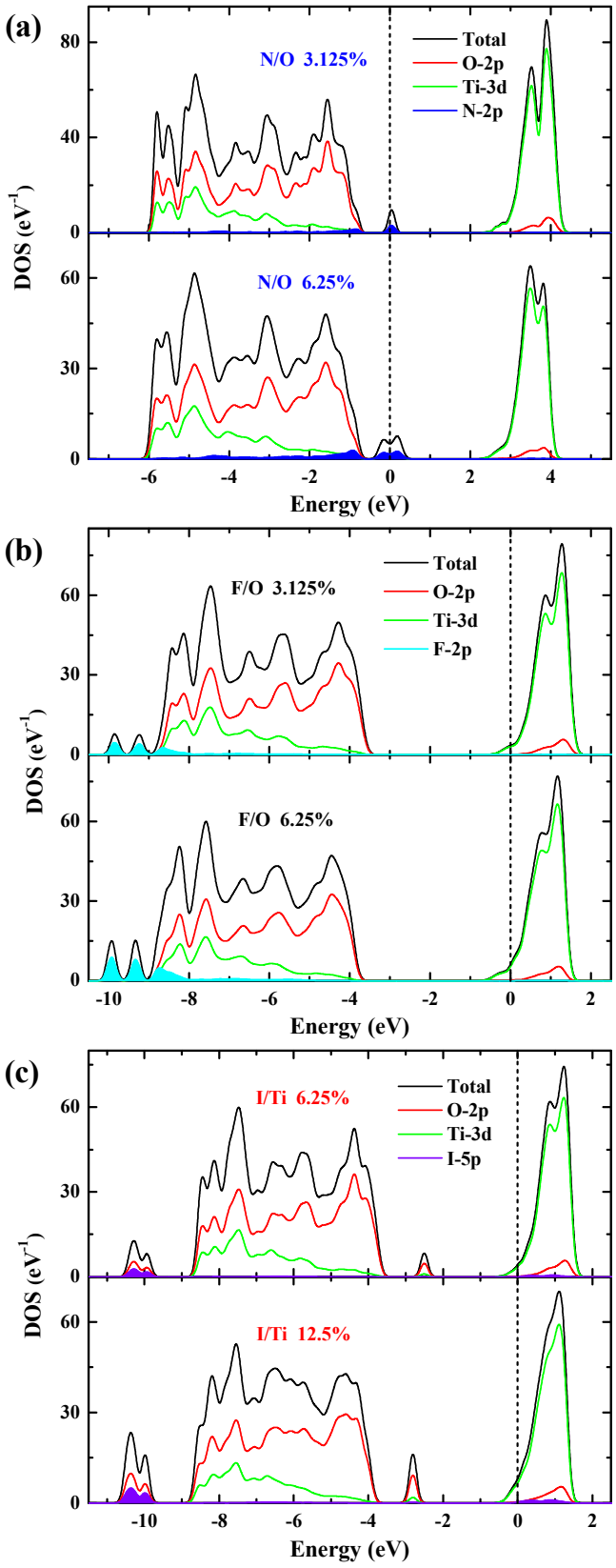
(a)
N/O 3.125%
N/O 6.25%
Total
O-2p
Ti-3d
N-2p
DOS (eV^{-1})
Energy (eV)
(b)
F/O 3.125%
F/O 6.25%
Total
O-2p
Ti-3d
F-2p
DOS (eV^{-1})
Energy (eV)
(c)
I/Ti 6.25%
I/Ti 12.5%
Total
O-2p
Ti-3d
I-5p
DOS (eV^{-1})
Energy (eV)

Figure S2. The HSE06 calculated DOSs for (a) N doped, (b) F doped, and (c) I doped anatase TiO_2 in the low and high doping concentration regime. The Fermi level of these systems is displayed with a black dashed line.